Prehistoric Fault Offsets of the Hilina Fault System, South Flank of Kilauea Volcano, Hawaii[1]

Eric C. Cannon, Department of Geology, One Shields Avenue, University of California, Davis, CA, 95616; phone: (530) 752-0350
e-mail: cannon@geology.ucdavis.edu

Roland Bürgmann, Department of Geology and Geophysics, 307 McCone Hall, University of California, Berkeley, Berkeley, CA 94720-4767; phone: (510) 643-9545
e-mail: burgmann@seismo.berkeley.edu

(submitted 05-17-00 to the *Journal of Geophysical Research*)

[1] More information available at http://perry.geo.berkeley.edu/~burgmann/RESEARCH/research.html

Abstract

Fault offsets in prehistoric dated lava flows characterize the past faulting behavior of the Hilina fault system. Historical accounts of earthquakes on Hawaii only date back to 1823 but lava flows as old 3000 yr B.P. still contain piercing points of prehistoric fault offsets (yr B.P. - radiocarbon years before present relative to 1950). We define a "Kalapana-type" earthquake as any large (M>7) earthquake that produces offsets along the Hilina fault system similar to fault offsets measured for the 1975 Kalapana earthquake. We compare fault offsets in prehistoric lava flows with fault offsets in neighboring 1969-1974 Mauna Ulu lava flows (Kalapana earthquake surface rupture) to estimate the past occurrence of prehistoric Kalapana-type earthquakes. Horizontal and vertical fault offset rate across the Hilina fault system are 4.0 to 12.0 mm/yr and -2.0 to -20.0 mm/yr respectively based on lava flows less than 750 yr B.P. age. Our best estimate of the number of Kalapana-type earthquakes to occur in lava flows 400-750 yr B.P. age is 3-5 events (260-80 year recurrence interval). Vertical fault offset values in prehistoric flows suggest hanging wall rotation of the Hilina fault system contributes to fault offset. Our assumption of a Kalapana-type earthquake is an over-simplification of past faulting events. Large south flank earthquakes most likely have non-uniform recurrence intervals.

Introduction

The south flank of Kilauea Volcano, Hawaii has experienced at least two large (M>7) earthquakes that ruptured a large subhorizontal detachment fault at the base of the volcanic edifice, the 1975 M7.2 Kalapana earthquake and 1868 M7.9 Great Kau earthquake (Figure 1) [*Ando*, 1979; *Furumoto and Kovach*, 1979*; Tilling et al*., 1975; *Lipman et al*., 1985; *Wyss*, 1988]. Estimates of recurrence intervals for these large earthquakes remain disputed [*Wyss and Koyanagi*, 1992]. Large south flank earthquakes pose a significant hazard to the Hawaiian Islands from catastrophic landslides and submarine slumps [*Lipman et al*., 1985*; Moore et al.*, 1995; *Ma et al.*, 1999]. Tsunamis from the 1975 Kalapana and 1868 Great Kau earthquake reached maximum heights of ~15 m and ~14 m respectively on the south flank coast. Tsunamis generated from future catastrophic south flank failures might threaten cities around the Pacific Rim.

This research focuses on evaluating past faulting behavior of the Hilina fault system associated with large south flank earthquakes. Records of historical seismicity on Hawaii date back to 1823 [*Wyss and Koyanagi*, 1992]. Evaluating the faulting behavior prior to historic accounts requires geologic field observations of surface deformation caused by large earthquakes. Triggered slip along the normal faults of the Hilina fault system recorded in prehistoric lava flows is the only accessible source of geologic information about prehistoric earthquakes. First, we document ground fractures from the 1975 Kalapana earthquake (hereafter referred to as the Kalapana earthquake), the only large south flank earthquake with available geodetic measurements of displacement, seismicity, and fault offset measurements along the Hilina fault system. Second, we compare the Hilina fault offsets associated with the Kalapana earthquake and the fault offsets in prehistoric dated lava flows to provide an estimate for the number of large earthquakes to have struck the south flank.

Characterizing the past faulting behavior of the Hilina fault system will be applicable to future earthquake, landslide, and tsunami hazard assessments of the south flank.

South Flank Tectonic Setting

Seismic and geodetic data from the Kalapana earthquake, distribution of microseismicity, and geological features help define the structural geometry of the south flank. The wedge-shaped mobile south flank block is bounded at ~8-10-km-depth by a shallowly landward-dipping basal detachment fault, illuminated by microseismicity beneath the upper south flank [*Ando*, 1979; *Got et al*., 1994; *Gillard et al*., 1996], and imaged offshore at shallower depths in seismic reflection data [*Morgan et al*., Confirmation of volcanic spreading models for Kilauea's mobile south flank, Hawaii, from marine seismic reflection data, in review to *Geology*, 1999, hereafter referred to as *Morgan et al.*, in review, 1999a; *Morgan et al.*, Paua'u seamount: the submarine expression of the active Hilina slump, south flank of Kilauea Volcano, Hawaii, submitted to *Journal of Geophysical Research*, 1999 hereafter referred to as Morgan et al., submitted manuscript, 1999b]. The basal detachment fault may develop along a weak boundary layer comprised of ocean sediments deposited on the Cretaceous ocean floor [*Hill*, 1969*; Nakamura*, 1980; *Thurber and Gripp*, 1988]. Focal mechanism studies of the Kalapana earthquake mainshock and its aftershock sequence indicate seaward transport of the south flank along the basal detachment fault [*Ando*, 1979; *Furumoto and Kovach*, 1979; *Gillard et al*., 1996].

The subaerial extent of the south flank is bounded to the north by Kilauea caldera and the Southwest and East rift zones (Figure 2). Lateral boundaries are not as well defined as subaerial boundaries. To the west, the Papa'u seamount submarine ridge does not continue onshore as a linear feature displaying right-lateral displacement

as might be expected for the western boundary of the south flank [*Chadwick et al*., 1993; *Denlinger and Okubo*, 1995]. The Papu'u seamount probably represents a fault-propagation fold produced by the active Hilina slump [*Morgan et al*., 1999b]. In the east, low electrical resistivity lineations interpreted as conductive zones above dikes may indicate lateral boundaries of large-scale slump structures [*Flanigan and Long*, 1987]. The southern extent of the south flank is represented by the distal toe of the Hilina slump 50-60 km offshore [*Lipman et al*., 1985; *Moore et al*., 1995; *Morgan et al*., 1999].

A combination of rift zone dike intrusions [*Fiske and Jackson*, 1972; *Swanson et al*., 1976*; Denlinger and Okubo*, 1995] and gravitational spreading [*Dieterich*, 1988; *Delaney et al*., 1998] probably displaces the south flank to the southeast. A variety of geodetic studies, including triangulation, trilateration, leveling, and Global Positioning System (GPS) measurements, have detected overall seaward motion of the south flank since 1896 [*Swanson et al*., 1976; *Lipman et al.* 1985; *Owen et al*., 1995; *Delaney et al*., 1998]. Geodetic station Panau ("P" in Figure 1) has moved seaward at least 10 m horizontally since 1896, with approximately 4 m horizontal displacement from the Kalapana earthquake and the remaining amount by aseismic slip along the basal detachment [*Swanson et al*., 1976]. However the Panau-Laeapuki baseline ("P-L" in Figure 1) shortened ~1 m from 1898 to 1970, indicating the coastal south flank was under compression prior to the Kalapana earthquake [*Swanson et al*., 1976]. Contraction of geodetic baselines across the south flank, except for extension during rift zone intrusions, occurred after the Kalapana earthquake until about 1981 [*Delaney et al*., 1998]. Baselines have showed continued extension since the January 1983 eruption of Puu Oo [*Delaney et al.*, 1998]. Between 1990 and 1996, GPS stations indicated south flank horizontal displacement rates of up to 10 cm/yr [*Owen et al*., 1995; *Owen et al*., 1999]. Models of observed displacement rates require 15-25 cm/yr slip on a 9-km-deep

horizontal detachment [*Owen et al*., 1995]. Whereas geodetic baselines across the south flank show significant extension and contraction since the Kalapana earthquake, baselines changes across the Hilina fault system suggest the Hilina faults have not significantly displaced except from the Kalapana earthquake [*Delaney et al.*, 1998].

The wedge-shaped mobile south flank is crosscut by the east-west trending Koae and Hilina normal fault systems (Figure 1). The Koae faults dip to the north and show 1-2 m opening with less than 20 m vertical offset [*Duffield*, 1975]. The Hilina morphological fault scarps dip seaward with up to 500 m vertical offset. Hilina faults may be deep-rooted normal faults splaying off the basal detachment [*Lipman et al*., 1985]. Seismic tomography studies from *Okubo et al*. [1997] show a steeply southeast-dipping lateral gradient in P-wave velocity down to 10 km depth beneath the Hilina fault system. This gradient is interpreted as the Hilina fault boundary between high velocity rocks of the volcanic edifice and low velocity hanging wall rocks of the Hilina fault system.

Alternatively, the Hilina faults are interpreted as shallow normal faults [*Swanson et al*., 1976; *Ando*, 1979; *Hill and Zucca*, 1987; *Gillard et al*., 1996]. *Riley* [1996] used paleomagnetic measurements from landward-rotated lava to estimate fault depth in the Hilina fault system. She modeled cylindrical slip on the Puu Kapukapu fault as a 5.2-km-deep fault. Fault offset measurements and geodetic data from the Kalapana earthquake suggest the Hilina faults are a set of shallow normal faults [*Cannon et al.*, Normal faulting and block rotation associated with the Kalapana earthquake, Kilauea Volcano, Hawaii, submitted to the *Bulletin of the Seismological Society of America*, 2000 hereafter referred to as *Cannon et al.*, submitted manuscript 2000]. *Morgan et al*. [1999b] interpreted some seismic reflectors offshore of the south flank as a possible 2-3-km-deep detachment to the Hilina fault system.

The Kalapana and Great Kau Earthquakes

The M7.2 Kalapana earthquake is the largest earthquake to strike the south flank in the twentieth century [*Tilling et al*., 1975; *Stover and Coffman*, 1993]. Over 25 km of surface rupture occurred along the Hilina faults with a maximum of 1.5 m vertical offset (Figure 1) [*Tilling et al*., 1975]. An estimated 1000 square kilometers of fault surface area ruptured on the basal detachment [*Lipman et al*., 1985]. Coastal geodetic stations displayed up to 8 m horizontal motion and 3.5 m vertical subsidence [*Tilling et al*., 1975; *Lipman et al*., 1985]. Approximately 60 km of coastline from Punaluu to Kaimu (Figure 1) subsided due to the Kalapana earthquake [*Lipman et al*., 1985].

The 1868 M7.9 Great Kau earthquake (hereafter referred to as the Great Kau earthquake) is one of the fifteen largest earthquakes recorded in the United States [*Stover and Coffman*, 1993] and the largest historical earthquake to occur in Hawaii (Figure 1). The earthquake sequence included a M~6.7 foreshock on 28 March 1868, the M7.9 mainshock on 2 April 1868, and possibly a decade of aftershock activity [*Wyss*, 1988]. A ~14 m high tsunami inundated coastal villages along the south flank coast [*Tilling et al*., 1975; *Wyss*, 1988; *Wyss and Koyanagi*, 1992]. *Brigham* [1909] reported 1.2 – 2.1 m of permanent coastal subsidence along ~80 km of coastline from Punaluu to Kapoho (Figure 1). *Wyss* [1988] estimated 8m of horizontal slip over a basal detachment area of 4000 square kilometers bounded by Mauna Loa rift zones.

Methods of Determining Fault Offsets and Time-Averaged Offset Rates

To improve our understanding of faulting behavior of the Hilina fault system prior to the Kalapana and Great Kau earthquakes, we measure Hilina fault offsets of historic and prehistoric lava flows. Fault offsets are measured from piercing points to

determine plunge, azimuth, and total length of offset. Then, total offset measurements are decomposed into horizontal and vertical components. We utilize GPS-RTK (Real-Time Kinematic) and post-processed differentially-corrected GPS equipment to record locations of fractures and fault offset. To measure a piercing point with GPS-RTK equipment, we record the locations of each end of the piercing point and then calculate the piercing point attitude. We use the measuring tape and compass technique for fault offsets in rugged terrain or remote field locations where GPS-RTK equipment is difficult to operate. We use a compass to obtain plunge and azimuth of the piercing point and total length is measured with a tape measure. We determine the location of the piercing point with a handheld GPS receiver and later post-process and differentially-correct the location. RTK equipment has an instrument error of 1-2 cm horizontal and 2-4 cm vertical for location positions, while the differentially-corrected post-processed GPS equipment has 1-2 m horizontal and 2-4 m vertical instrument error for locations. We estimate our horizontal and vertical measurement error in obtaining a piercing point attitude with the measuring tape and compass technique to be ±1 cm.

Fault offset measurements across a fault zone are collected in traverses conducted perpendicular to main fault traces of the Hilina faults (Figure 3d). Fault offset does not occur on one major fracture but rather throughout a zone of fractures. For each traverse, individual fault offsets are summed to calculate total fault offset for the traverse. For example, individual horizontal measurements of fault offset "a" through "k" (11 measurements) are summed to produce horizontal fault offset T53. Vertical measurements for a traverse are calculated using the same method. 73 traverses along the Hilina fault system contain over 700 measurements. Error bounds

for fault offset traverses containing multiple piercing point offsets are calculated as the $\sqrt{(\sum \text{ of the (measurement errors)}^2)}$ convention.

Time-averaged calculations for fault offset rates require offset measurements recorded in dated lava flows. We use ages for south flank lava flows given in radiocarbon year ages (Figure 4). *Wolfe and Morris* [1996] utilized several methods to date lava flows including observed stratigraphic relationships, alteration of lava flow surfaces from an initially glassy surface, radiocarbon ages from charcoal samples [*Lipman and Lockwood*, 1980], and paleomagnetic secular variation [*Holcomb*, 1987]. Radiocarbon years are defined as "years before present relative to 1950" represented by the symbol "yr B.P." Ages of south flank lava flows include 200-750 yr B.P., 400-750 yr B.P., 750-1500 yr B.P., and 1500-3000 yr B.P. from *Wolfe and Morris* [1996]. Two lava flows have ages of 350-450 yr B.P. and 2350-2450 yr B.P. determined using radiocarbon dating methods [D. A. Swanson, 2000, personal communication]. Given a lava flow of known age, a minimum time-averaged offset rate is calculated by dividing the fault offset for a given traverse by known age of the lava flow containing the traverse. This time-averaged calculation is a theoretical minimum fault offset rate because fault offsets probably occurred sometime after the lava flow cooled.

Kalapana Earthquake Ground Fracture and Fault Offset Data

The first step in understanding past faulting behavior of the Hilina fault system requires study of the ground fracture and fault offsets of the Kalapana earthquake. We present the first ground fracture map for the Kalapana earthquake (Figure 3b-e). Mauna Ulu lava flows (1969-1974) cover the central south flank region in pahoehoe and aa flows. These flows were fractured along the Hilina faults during the Kalapana

earthquake [*Cannon et al.*, submitted manuscript 2000]. Single fractures extend as far as 170 m in length and fracture zones span a width of up to 200 m (Figure 3b). Fault ramps and steps produce fractures distributed throughout the fracture zone, not necessarily concentrated at the northern or southern boundaries of the fracture zone (Figure 3b-e).

To determine fault offset of the Hilina fault system associated with the Kalapana earthquake, we present fault traverses in Mauna Ulu lava flows (solid vectors in Figure 5). Maximum horizontal and vertical fault offset occur on the Holei Pali fault, with 2.8 m of horizontal offset and 1.6 m of vertical offset determined from summing 16 individual piercing point measurements. For each traverse, we define the plunge of the slip vector as the arctangent of vertical fault offset divided by horizontal fault offset. We use the plunge of the slip vector as a proxy for the fault angle of the normal faults (Table 1). The average plunge of slip vectors for traverses across the Poliokeawe Pali, Holei Pali, and Apua Pali faults are 23°±24°, 23°±07, and 13°±15° respectively. For all plunges of slip vectors for the Hilina fault system, the average plunge is 20°±17°.

Fault Offsets in Prehistoric Lava Flows

We measure the Hilina fault offsets in prehistoric lava flows (open vectors in Figure 5) to extend our knowledge about south flank earthquakes as far back as 1500-3000 yr B.P. We are interested in determining fault offsets and fault offset rate for individual faults and across the Hilina fault system. Quality of fault offset preservation decreases with increased flow age. Lava flows less than 750 yr B.P. age preserve sawtooth-shaped fractures and produce piercing points that can be easily measured. Lava flows with ages greater than 750 yr B.P. have degraded fracture surfaces that make fault offset measurements difficult or impossible to obtain. Often with flows older than

750 yr B.P., only estimates of scarp height are obtained with error estimates of a few meters. When a piercing point is not preserved, no measurement of horizontal or vertical fault offset can be determined.

To estimate the number of large earthquakes that have occurred on Hilina faults, we collect offset data at locations with two important requirements. First, prehistoric lava flows and Mauna Ulu flows must be juxtaposed. Second, fault offsets in prehistoric lava flows must be well-preserved for measurement of piercing points. The Kealakomo Overlook region meets both of these requirements (Figure 6). The Mauna Ulu lava flows are bounded to the east and west by 400-750 yr B.P. age lava flows. Traverses span both the Poliokeawe Pali and Holei Pali with traverses A and D located in the prehistoric lava flows, and traverses B and C located in the Mauna Ulu lava flows. Fault offsets in the Mauna Ulu lava flows display 1-2 m horizontal offset and 0.2-0.5 m vertical offset. Fault offsets in the prehistoric lava flows show 2-3 m horizontal fault offset and 3-4 m vertical fault offset.

Analyzing fault offsets relationships at double-fracture outcrop locations is another method used to estimate the occurrence of large earthquakes. We define a double-fracture outcrop in three stages using the following example. First, a prehistoric lava flow of known age has been offset perhaps multiple times by prehistoric earthquakes. Second, Mauna Ulu lava flows infilled the prehistoric fracture between 1969 and 1974. Third and most recently, faulting of the Hilina fault system in the Kalapana earthquake produced a fault offset across the fracture. We measure the piercing point contained in the Mauna Ulu flow and a piercing point identified in the prehistoric lava flow. We then compare total fault offset in the prehistoric lava flow with fault offset from the Kalapana earthquake in the Mauna Ulu lava flow to estimate the recurrence of large earthquakes. Double-fracture outcrops are identified at three locations in the Hilina fault system (lettered locations in Figure 4). Total fault offsets in

Mauna Ulu flows vary from 5-67 cm while total fault offsets in prehistoric lava flows vary from 80-89 cm (Table 2).

We evaluate the time-averaged slip rate for the Hilina faults using three methods: (1) rate calculation for each individual traverse; (2) average rate on a single fault; (3) total rate across the Hilina fault system. Time-averaged fault offset rates for individual traverses in prehistoric lava flows are presented in Figure 7. Fault offset data from prehistoric lava flows (Figure 5) divided by age of lava flow produces a fault offset rate for each traverse. Solid vectors indicate locations with both horizontal and vertical fault offset measurements whereas open vectors and white dots indicate traverses lacking horizontal or vertical fault offset measurements. This figure simplifies south flank faults and lava flow geometry and preserves spatial relationships between lava flows and faults. Considering fault offsets in lava flows for ages back to 1500-3000 yr B.P., maximum horizontal and vertical fault offset rates are approximately 10 mm/yr and -20 mm/yr respectively. A negative vertical fault offset rate indicates hanging wall down motion.

Average fault offset rates calculated for the Poliokeawe Pali, Holei Pali, and Apua Pali faults are presented in Figure 8. The Poliokeawe Pali and Holei Pali faults display greater horizontal and vertical fault offsets than compared to values for the Apua Pali fault. For these three faults, the maximum average horizontal fault offset rate for fault offsets in lava flows less than 750 yr B.P. is 0.46 mm/yr for the Holei Pali fault, and the Poliokeawe Pali displays the maximum vertical fault offset rate -0.56 mm/yr (open symbols in Figures 8a and 8b). A negative vertical offset rate indicates hanging wall down fault offset. Horizontal and vertical fault offset rates on the Holei Pali fault based on a lava flow of age 750-1500 yr B.P. (solid symbol in Figures 8a and 8b) falls between of range of values calculated for fault offset rates in younger lava flows.

To evaluate fault slip and fault slip rates across the entire Hilina fault system, we select multiple traverses that descend across the Hilina fault system on a lava flows of

the same known age (Figure 9a). Eight traverses (#1-#8) extend generally north-south across the Hilina fault system. Traverse #1 occurs in a lava flow of age 2350-2450 yr B.P., traverses #2 and #3 in lava flows of 1500-3000 yr B.P. age and 750-1500 yr B.P. age respectively, and traverses #4-#8 in lava flows of 200-750 yr B.P. age. For south flank lava flows of less than 750 yr B.P. age, the maximum horizontal fault offset is 7±2 m and the maximum vertical fault offset is 10±1 m (Figures 9b and 9c). For lava flows less than 750 yr B.P. age, fault offset rates across the Hilina fault system range from 4.0 to 12.0 mm/yr and -2.0 to -20.0 mm/yr for horizontal and vertical fault offset rates respectively (Figures 9b and 9c). Horizontal fault offset rates for lava flows greater than 750 yr B.P. age fall below the minimum value of 4.0 mm/yr based on lava flow ages of less than 750 yr B.P. Vertical fault offset rates in lava flows greater than 750 yr B.P. exist in the range of fault offset values for lava flow less than 750 yr B.P.

Discussion

We now evaluate the past faulting behavior of the Hilina fault system by discussing our observations and analysis of fault offset measurements for fractures contained in prehistoric and the Mauna Ulu lava flows. We characterize the past faulting behavior of the Hilina faults by (1) interpreting ground fractures from the Kalapana earthquake; (2) comparing slip vectors associated with the Kalapana earthquake and prehistoric offsets; (3) discussing slip rates calculated for individual traverses, individual Hilina faults, and across the Hilina fault system to show possible hanging wall rotation; (4) establishing an initial estimate of the number of large (M>7) earthquakes to have occurred in the last ~3000 years; and (5) discussing our assumption of a characteristic Kalapana-type earthquake in (4).

We interpret the formation of fractures in Mauna Ulu flows associated with the Kalapana earthquake as tectonic in origin. Compressional fold and fault structures are

not observed at the base of fault scarps, indicating mass movements did not produce the fractures. Where fractures are wide enough to climb down, we examine the fracture walls for piercing points and subsurface detachment surfaces parallel to the base of flows. No subsurface detachment surfaces are observed on fracture walls, suggesting the upper few meters of lava flow did not detach from the subsurface to produce fractures observed at the surface.

Kalapana earthquake and prehistoric fault offsets display similar slip vectors. Comparing azimuths of slip vectors, horizontal offsets in Mauna Ulu flows (solid vectors in Figure 5) show motion toward the southeast in agreement with the overall southeast direction of south flank transport for the Kalapana earthquake [*Tilling et al*., 1975; *Lipman et al*., 1985]. Horizontal fault offsets for both Mauna Ulu and prehistoric lava flows (open vectors in Figure 5) generally trend southeast, but the local trend of the fault trace seems to constrain fault offsets to be in a fault-perpendicular direction [*Cannon et al.*, submitted manuscript 2000]. Considering the plunges of slip vectors, the average plunge of slip vectors for Hilina faults from the Kalapana earthquake is 20°±17° whereas prehistoric lava flows show 31°±23°. Plunges of slip vectors for Kalapana earthquake offsets and prehistoric fault offsets suggest that the fault surfaces of the Hilina fault system have an overall dip of less than 45°. Shallow plunges of slip vectors confirm that the Hilina fault system consists of a series of shallow normal slide blocks rather than deep normal faults [*Cannon et al*., submitted manuscript 2000].

Prehistoric fault offset and slip rate values show evidence for hanging wall rotation of the Hilina fault system. For individual traverses (Figure 7), the maximum vertical fault offset rate is approximately -20 mm/yr, twice the value for maximum horizontal fault offset rates. Taking the average fault offset rate for individual faults, the Holei Pali fault has a greater vertical fault offset rate than horizontal value (Figure

8). However, both the Poliokeawe Pali and Apua Pali faults have horizontal average fault offset rates greater than average vertical values. Traverses across the Hilina fault system show for lava flows greater than 750 yr B.P. age, vertical fault offsets are greater than horizontal values (Figure 9). For traverses in lava flows less than 750 yr B.P. age, vertical fault offsets are mostly greater than or equal to horizontal values.

Whereas fault offsets from the Kalapana earthquake were predominantly horizontal (solid vectors in Figure 5), fault offsets and fault offset rates in prehistoric lava flows show an increased or dominant contribution of vertical fault offset to total fault offset. We suggest that the dominance of vertical offset in prehistoric lava results from progressive block rotation of the hanging walls of the Hilina fault system [*Cannon et al*., submitted manuscript 2000]. Surface lava flows fractured by only one earthquake (i.e. Mauna Ulu flows fractured in the Kalapana earthquake) will show predominantly horizontal fault offset. As time progresses, incremental block rotation from multiple earthquakes will increase values of vertical fault offset observed on fractures.

We estimate the number of large earthquakes and their time-averaged recurrence intervals that might have occurred for the Poliokeawe Pali and Holei Pali at Kealakomo Overlook (Figure 6). Comparing the Kalapana earthquake fault offset traverse B to 400-750 yr B.P. age fault offset traverse A, 3-5 Kalapana-type earthquakes could have produced fault offsets observed in the 400-750 yr B.P. age lava flows. The time-averaged recurrence interval for Kalapana-type earthquakes on fault offset traverses A and B is 260-80 years. Horizontal fault offsets are about equal for traverses C and D; fault offsets from the Kalapana earthquake and prehistoric offsets respectively. However, vertical fault offset in traverse D may be explained by as many as seven Kalapana-type fault offsets, measured in traverse C. Large error bars on fault offset traverse D result from poor scarp preservation. 3-5 Kalapana-type earthquakes can

explain offsets in prehistoric flows observed in traverse B, but as few as one and as many as seven Kalapana-type earthquakes may have produced offsets in traverse C. We place more confidence in interpretations of the number of Kalapana-type earthquakes and recurrence intervals calculated from traverses A and B, than traverses C and D, due to poor offsets located along traverse D.

Interpreting fault offsets at double-fracture outcrops also provides estimates for the number of past large earthquakes and recurrence intervals (Table 2). Assuming multiple Kalapana-type earthquakes produced the total fault offset observed in the prehistoric lava flow, 1.2-17.5 Kalapana-type earthquakes with time-averaged recurrence intervals of 650 to 20 years may have occurred on the Hilina faults. The wide range of the number of estimated Kalapana-type earthquakes may be due to unique fault offsets on each fault for each event, rather than a uniform fault offset for each event. The large variance in time-averaged recurrence intervals suggests that large south flank earthquakes may not produce a uniform fault offset on Hilina faults with each event. Since double-fracture outcrops may be greatly influenced by local faulting characteristics, time-averaged recurrence intervals calculated from fault traverses spanning multiple fractures (i.e. Kealakomo Overlook) provide a more confident value.

Our recurrence interval estimates from double-fracture outcrops and Kealakomo Overlook agree with values determined in previous studies. Estimating a recurrence interval for large south flank earthquakes remains difficult since only the Great Kau and Kalapana earthquakes have been documented. From the time interval between the 1868 Great Kau and 1975 Kalapana earthquakes, the recurrence interval for a $7<M<8$ earthquake in the Kalapana area is 108 years [*Wyss and Koyanagi*, 1992]. *Lipman et al.* [1985] concluded approximately 1000 Kalapana earthquake subsidence events may be responsible for the Hilina fault scarp morphology. Given 23 ky as the minimum age

estimate for Hilina faults [*Easton*, 1978 – age of Pahala ash cap on Puu Kapukapu], a 230 year recurrence interval is obtained. *Riley* [1996] determined from paleomagnetic landward rotations of the block bounded by the Puu Kapukapu and Hilina faults a recurrence interval of 200 years.

Caution must be exercised with these recurrence interval estimates of large earthquakes in a volcanic system. Time-averaged recurrence intervals are based on Hilina fault offset due to the Kalapana earthquake, not from the absolute ages of multiple earthquake events. Volcanic processes and changes through time, such as changes in magma transport, may play an important role in developing and triggering a large earthquake and producing non-uniform recurrence intervals. Whereas plate boundary earthquakes may be due to steady loading at the plate boundaries, volcanic systems have loading events that vary drastically on all timescales. The 1975 Kalapana and 1868 Great Kau earthquakes were two very different events which brings into question the assumption we and others have made about a Kalapana-type "characteristic" earthquake.

Our estimates of the number of past large south flank earthquake and recurrence interval calculations depend on the main assumption that all past large earthquakes produced fault offsets comparable to fault offsets measured in the Hilina fault system for the Kalapana earthquake. The wide range of recurrence interval estimates and number of large earthquakes suggest slip on Hilina fault systems is not uniform and periodic for past earthquakes. Fault offsets at Kealakomo Overlook and the Poliokeawe double-crack outcrop (location "a" in Figure 4 and Table 2) might be explained by as few as two earthquake events in the last 400-750 yr B.P., the Kalapana earthquake, and the Great Kau earthquake. We speculate that the larger magnitude Great Kau earthquake may have produced more slip on the Hilina fault system than occurred with the

Kalapana earthquake. Fault offsets of 400-750 yr B.P. age lava flows on the Poliokeawe Pali might have been produced by only the Great Kau and Kalapana earthquakes, again suggesting that large south flank earthquakes do not have uniform repeat times.

Conclusions

Detailed mapping of the 1975 Kalapana surface rupture and the fault offsets in prehistoric flows allow us to characterize the past faulting behavior of the Hilina fault system. Accounts of historical earthquakes on Hawaii only date back to 1823, but we extend the earthquake record as far back as 1500-3000 yr B.P by comparing fault offsets in prehistoric lava flows with neighboring Kalapana earthquake fault offsets.

We draw several conclusions about past faulting behavior of the Hilina fault system from our fault offset analysis. We focus our conclusions on prehistoric lava flows as far back as 750 yr B.P. age since these lava flows best preserve piercing points. Average plunges of slip vectors for the Kalapana earthquake and fault offsets in prehistoric lava flows are 20°±17° and 31°±23° respectively indicating the Hilina faults are probably shallow normal faults rather than steep and deep-rooted normal faults. Fault offset rates for individual Hilina faults are up to 0.46 mm/yr and up to -0.56 mm/yr for horizontal and vertical rates respectively. Horizontal and vertical fault offset rates across the entire Hilina fault system are 4.0 to 12.0 mm/yr and -2.0 to -20.0 mm/yr respectively. Vertical components of fault offset in prehistoric lava flows probably increase over time due to hanging wall rotation of the Hilina fault system If we assume each prehistoric faulting event has "Kalapana-type" fault offsets equal to measured Kalapana earthquake fault offsets on the Hilina faults, the number of large earthquakes to occur as far back as 750 yr B.P. ranges from 1.2 to 17.6, with recurrence

intervals of 650-20 years. Our best estimate suggests that 3-5 "Kalapana-type" events have occurred with recurrence intervals of 260-80 years.

The wide range of estimates on the number of prehistoric faulting events suggests that these events do not necessarily produce Kalapana-type offsets. Prehistoric fault offsets of age less than 750 yr B.P. may be explained by just two earthquakes, the 1975 Kalapana and 1868 Great Kau earthquakes. Fault offsets of prehistoric earthquakes probably are not uniform for each event and these earthquakes do not have uniform recurrence intervals. Our work supplies crucial fault offset information to improve earthquake hazard assessment of the south flank. However, our efforts are limited to the Mauna Ulu lava flows and prehistoric lava flows that have preserved piercing points. Geodetic monitoring of strain accumulation across the south flank and seismic monitoring are better suited to directly evaluate future earthquake hazards on the south flank.

Acknowledgements

This work was supported by a U. S. Geological Survey National Earthquake Hazards Reduction Program grant 14534-HQ-98-GR-1024, a Geological Society of America Student Research grant (E.C.C.), and a University of California, Davis Cordell Durrell grant (E.C.C.). James McClain and Robert Twiss provided comments to significantly improve this manuscript. We received help from many people at the Hawaiian Volcano Observatory, especially Don Swanson, Michael Lisowski, Asta Miklius, Kristine Larson, Taeko Jane Takahashi, Arnold Okamura, Richard Fiske, and Paul Okubo. We thank James Kellogg and William Chadwick for provided fault offset data and field notes from their Hilina fieldwork. We appreciate the excellent efforts of our field assistants Jason Bariel, Chad Fleschner, Mike Poland, Gwen Pikkarainen, and

Jim Weigel. Many figures were produced with Generic Mapping Tool software [*Wessel and Smith*, 1995].

References Cited

Ando, M., The Hawaii earthquake of November 29, 1975: low dip angle faulting due to forceful injection of magma, *J. Geophys. Res.*, 94, no. B13, 7616-7626, 1979.

Brigham, W. T., The volcanoes of Kilauea and Mauna Loa on the island of Hawaii, *Memories of the Bernice Pauahi Bishop Museum*, 2, 478-497, 1909.

Cannon, E. C., R. Bürgmann, and S. E. Owen, Normal faulting and block rotation associated with the Kalapana earthquake, Kilauea Volcano, Hawaii, *Bull. Seismol. Soc. Amer.*, 2000 (submitted for publication).

Chadwick Jr., W. W., J. R. Smith Jr., J. G. Moore, D. A. Clague, M. O. Garcia, and C. G. Fox, Bathymetry of south flank of Kilauea Volcano, *U.S. Geol. Surv. Misc. Field Studies*, map MF-2231, 1993.

Delaney, P. T., R. Denlinger, M. Lisowski, A. Miklius, P. Okubo, A. Okamura, and M. K. Sako, Volcanic spreading at Kilauea, 1976-1996, *J. Geophys. Res.*, 103, no. B8, 18003-18023, 1998.

Denlinger, R. P. and P. Okubo, Structure of the mobile south flank of Kilauea, Volcano, Hawaii, *J. Geophys. Res.*, 100, no. B12, 24499-24507, 1995.

Dieterich, J. H., Growth and persistence of Hawaiian volcanic rift zones, *J. Geophys. Res*., 93, 4258-4270, 1988.

Duffield, W. A., Structure and origin of the Koae fault system, Kilauea Volcano, Hawaii, *U.S. Geol. Surv. Prof. Pap. 856*, 1975.

Easton, R. M., The stratigraphy and petrology of the Hilina Formation; the oldest exposed lavas of Kilauea Volcano, Hawaii, M.S. thesis, Univ. of Hawaii, 1978.

Fiske, R. S. and E. D. Jackson, 1972, Orientation and growth of Hawaiian volcanic rifts: the effect of regional structure and gravitational stresses, *Royal Soc. London Proc*., 329, 299-326, 1972.

Flanigan, V. J. and C. L. Long, Aeromagnetic and near-surface electrical expression of the Kilauea and Mauna Loa volcanic rift systems, *U.S. Geol. Surv. Prof. Pap. 1350*, 935-946, 1987.

Furumoto, A. S., and R. L. Kovach, The Kalapana earthquake of November 28, 1975: an intra-plate earthquake and its relation to geothermal processes, *Phys. Ear. Plan. Int.*, 18, 197-208, 1979.

Gillard, D., M. Wyss, and P. Okubo, Type of faulting and orientation of stress and strain as a function of space and time in Kilauea's south flank, Hawaii, *J. Geophys. Res.*, 101, no. B7, 16025-16042, 1996.

Got, J.-L., F. W. Fréchet, and W. Klein, Deep fault plane geometry inferred from multiplet relative relocation beneath the south flank of Kilauea, *J. Geophys. Res.*, 99, no. B8, 15375-15386, 1994.

Hill, D. P., Crustal structure of the island of Hawaii from seismic-refraction measurements, *Bull. Seismol. Soc. Amer.*, 59, no. 1, 101-130, 1969.

Hill, D. P. and J. J. Zucca, Geophysical constraints on the structure of Kilauea and Mauna Loa Volcanoes and some implications for seismomagnetic processes, *U.S. Geol. Surv. Prof. Pap. 1350*, 903-917, 1987.

Holcomb, R. T., Eruptive history and long-term behavior of Kilauea Volcano, *U.S. Geol. Surv. Prof. Pap. 1350*, 261-350, 1987.

Lipman, P. W., J. P. Lockwood, R. T. Okamura, D. A. Swanson, and K. M. Yamashita, Ground deformation associated with the 1975 magnitude-7.2 earthquake and resulting changes in activity of Kilauea Volcano, Hawaii, *U.S. Geol. Surv. Prof. Pap. 1276*, 1985.

Ma, K.-F., H. Kanamori, and K. Satake, Mechanism of the 1975 Kalapana, Hawaii, earthquake inferred from tsunami data, *J. Geophys. Res*, 104, no. B6, 13153-13167, 1999.

Moore, J. G., W. B. Bryan, M. H. Beeson, and W. R. Normark, Giant blocks in the South Kona landslide, Hawaii, *Geology*, 23, 125-128, 1995.

Morgan, J. K., G. F. Moore, D. J. Hill, and S. Leslie, Confirmation of volcanic spreading models for Kilauea's mobile south flank, Hawaii, from marine seismic reflection data, *Geology*, 1999a (in review).

Morgan, J. K., G. F. Moore, and D. A. Clague, Papu'u seamount: the submarine expression of the active Hilina slump, south flank of Kilauea Volcano, Hawaii, *J. Geophys. Res*., 1999b (submitted manuscript).

Nakamura, K., Why do long rift zones develop better in Hawaiian volcanoes? A possible role of thick ocean sediment, *Bull. Volcano. Soc. Japan*, 25, 255-269.

Okubo, P. G., H. M. Benz, and B. A. Chouet, Imaging the crustal magma sources beneath Mauna Loa and Kilauea volcanoes, Hawaii, *Geology*, 25**,** no. 10, 867-870, 1997.

Owen, S., P. Segall, J. Freymueller, A. Miklius, R. Denlinger, T. Árnadóttir, M. Sako, and R. Bürgmann, Rapid deformation of the south flank of Kilauea Volcano, Hawaii, *Science*, 267, 1328-1332, 1995.

Owen, S., P. Segall, M. Lisowski, A. Miklius, R. Denlinger, J. Freymueller, T. Árnadóttir, and M. Sako, The rapid deformation of Kilauea Volcano: GPS measurements between 1990 and 1996, *J. Geophys. Res*., 1999 (in press).

Riley, C., A paleomagnetic study of movement in the Hilina fault system, south flank of Kilauea Volcano, Hawaii, M.S. thesis, Mich. Tech. Univ., 1996.

Stover, C. W. and J. L. Coffman, Seismicity of the United States, 1568-1989 (Revised), *U.S. Geol. Sur. Prof. Pap. 1527*, 1993.

Swanson, D. A., W. A. Duffield, and R. S. Fiske, Displacement of the south flank of Kilauea Volcano: the result of forceful intrusion of magma into the rift zones, *U.S. Geol. Surv. Prof. Pap. 963*, 1974.

Thurber, C. H. and A. E. Gripp, Flexure and seismicity beneath the south flank of Kilauea volcano and tectonic implications, *J. Geophys, Res.*, 93, 4271-4281, 1988.

Tilling, R. I., R. Y. Koyanagi, P. W. Lipman, J. P. Lockwood, J. G. Moore, and D. A. Swanson, Earthquake and related catastrophic events Island of Hawaii, November 29, 1975: A preliminary report, *U. S. Geol. Surv. Circ. 740*, 1976.

Wessel, P. and W. H. F. Smith, New version of the Generic Mapping Tools released, *EOS Trans., AGU,* 76, 329, 1995.

Wolfe, E. W. and J. Morris, Geologic map of the Island Of Hawaii, *U.S. Geol. Surv. Misc. Invest. Ser. Map I-2524-A,* 1996.

Wyss, M., A proposed source model for the Great Kau, Hawaii, earthquake of 1868, *Bull. Seismol. Soc. Amer.,* 78, no. 4, 1450-1462, 1988.

Wyss, M. and R. Y. Koyanagi, Seismic gaps in Hawaii, *Bull. Seismol. Soc. Amer.,* 82, no. 3, 1373-1387, 1992.

Figures

Figure 1. Location map for south flank of Kilauea Volcano, Hawaii. Stars locate epicenters for 1975 Kalapana and 1868 Great Kau earthquakes. Heavy dashed line indicates region of coastal subsidence for Kalapana earthquake from Punaluu to Kaimu; coastal subsidence from Great Kau earthquake probably extended further northeast (heavier bold line) to Kapoho [*Wyss,* 1988]. Abbreviations represent: KFS, Koae fault system; HFS, Hilina fault system; ERZ, east rift zone; SWRZ, southwest rift zone. Rupture of Hilina fault system in Kalapana earthquake shown with bold lines [*Lipman et al.*, 1985]. (P-L) represents Panau-Laeapuki geodetic baseline.

Figure 2. Shaded relief map of topography and bathymetry for south flank (digital topographic and bathymetric data provided by J. Smith [*Chadwick et al*., 1993]). Artificial illumination from the northwest. Heavy black lines indicate trace of Hilina fault system (HFS). Two outlined white regions indicate areas of low electrical resistivity [*Flanigan and Long*, 1987]. Open arrow indicates motion of Hilina slump towards western boundary; solid arrow indicates more southeast-directed motion of south flank; long-dashed solid line represents western boundary of Hilina (from *Morgan et al*. [1999]). Solid dashed lines with triangles indicate distal extent of hanging wall for south flank; short-dashed solid line may represent eastern boundary.

Figure 3. Location map for 1975 Kalapana earthquake ground fractures. (a) Lava flows of central Hilina fault system, ages defined in Figure 4. In all figures, Chain of Craters Road labeled (CoC). Lettered boxes in (a) show locations of Kalapana earthquake fractures on the (b) Poliokeawe Pali, (c) Poliokeawe & Holei Pali, (d) Holei Pali, and (e) Apua Pali faults. (d) Example of method to calculate fault offset traverses across a fault scarp: horizontal fault offset vector T53 (open vector) is sum of individual

horizontal fault offset measurements "a" through "g" (solid vectors). Scale vector for both solid and open vectors is 25 cm.

Figure 4. Geologic map of south flank of Kilauea Volcano, Hawaii. Map modified from *Wolfe and Morris* [1996]. Lettered locations a-c identify double-fracture outcrop locations (Table 2). Chain of Craters Road labeled (CoC).

Figure 5. Maps of (a) vertical fault offsets and (b) horizontal fault offsets along Hilina fault system. For (a) and (b) solid vectors indicate fault offsets in 1969-1974 Mauna Ulu lava flows, open vectors indicate fault offsets in prehistoric lava flows (ages defined in Figure 4), scale vector is 5 m with measurement error bounds shown; Chain of Crater Road labeled (CoC). South-trending vectors in (b) indicate hanging wall down fault offset.

Figure 6. Location map and graph of fault offsets at Kealakomo Overlook site. Chain of Craters Road labeled (CoC).

Figure 7. Diagram of (a) horizontal and (b) vertical fault offset rates from prehistoric lava flows; lava flow ages from Figure 4; error bounds indicate error propagated from fault offset traverses and lava flow ages. Although not to scale, diagrams preserve spatial relationships between lava flows and faults. Solid vectors indicate locations with both horizontal and vertical fault offset measurements; open vectors and white dots identify locations without both measurements; star indicates location of Kealakomo Overlook. South-trending vectors in (b) indicate hanging wall down fault offset.

Figure 8. Graphs of average horizontal (a) and vertical fault offsets (b) (from Figure 5b and 5a) verses lava flow age (from Figure 4) for individual fault offset traverses along Hilina fault system. Open symbols indicate lava flow ages less than 750 yr B.P.; solid symbol is for lava flow of 750-1500 yr B.P. age. Abbreviations represent:

A, Apua Pali; H, Holei Pali; P, Poliokeawe Pali; OH, Holei Pali (750-1500 yr B.P. lava flow). Horizontal error bars indicate range of lava flow age estimate; vertical error bars are standard deviation of average fault offsets. Slope of dashed line represent fault offset rates. Negative slope indicates hanging wall down fault offset.

Figure 9. (a) Map of traverse locations (dots; data from Figure 5) to construct fault offset traverses across the Hilina fault system. White dots connected with white lines represent traverses on lava flows older than 750 yr B.P., black dots connected with black lines indicate traverses on lava flows younger than 750 yr B.P. Lava flows for traverses are: #1, 2350-2450 yr B.P.; #2, 1500-3000 yr B.P.; #3, 750-1500 yr B.P. ; #4, 330-470 yr B.P.; #5, 200-750 yr B.P.; #6-#8, 400-750 yr B.P (lava flow ages from Figure 4). (b) and (c) Horizontal and vertical offset across Hilina fault system. Slope of dashed lines represent envelope of possible fault offset rates. Numbered symbols correspond to traverse numbers in (a). Horizontal error bars indicate age range of lava flow age estimate, vertical error bars indicate measurement error of fault offset and range of summed offset values. Negative slope indicate hanging wall down fault offset.

Table 1. Average Plunge Of Slip Vectors From Fault Traverses Across Hilina Fault System

Earthquake(s)	Poliokeawe Pali	Holei Pali	Apua Pali	All faults
Kalapana	23°±24°; n=12	23°±07°; n=15	13°±15°; n=9	20°±17°; n=36
Prehistoric	44°±27°; n=8	26°±18°; n=12	20°±14°; n=2	31°±23°; n=22

Note: average slip vectors format $\mu \pm 1\text{-}\sigma$; n
(μ) mean angular direction
(σ) mean angular deviation
(n) number of measurements from Figure 5

Table 2. Summary Of South Flank Double-Fracture Locations

Location *	Mauna Ulu Flow	Older Flow			
	1975 Offset (cm)§	Total Offset (cm)	C-14 age# (yr B.P.)	Number of Kalapana Events**	Recurrence interval(yrs)§§
A-Poliokeawe Pali	29	90	350-450	3.1	120-150
B-Holei Pali	67	80	200-750	1.2	190-650
C-Apua Pali	5	89	400-750	17.5	20-40

Notes: * See Figure 4 for location

§ Total offset assumed from 1975 Kalapana earthquke

Add 25 yrs for age relative to 1975 Kalapana earthquke

$$^{**}\text{Number of Kalapana Events} = \frac{\text{Total offset from prehistoric lava flow}}{\text{Total offset fromMauna Ulu lava flow}}$$

$$\S\S\text{Recurrence Interval [upper limit]} = \frac{\text{Upper value for C-14 age relative to Kalapana earthquake}}{\text{Number of Kalapana-type events}}$$

$$\S\S\text{Recurrence Interval [lower limit]} = \frac{\text{Upper value for C-14 age relative to Kalapana earthquake}}{\text{Number of Kalapana-type events}}$$

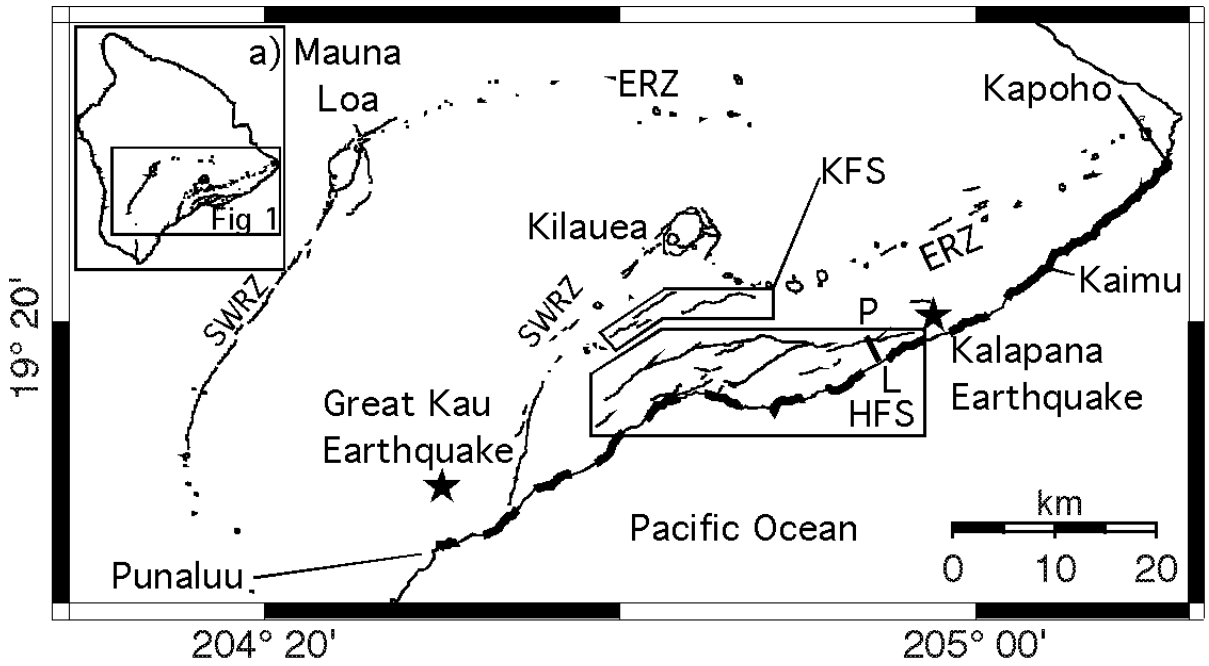
a) Mauna
Loa
Fig 1
ERZ
Kapoho
KFS
Kilauea
ERZ
Kaimu
SWRZ
SWRZ
P
Kalapana
Earthquake
L
HFS
Great Kau
Earthquake
Pacific Ocean
km
0 10 20
Punaluu
19° 20'
204° 20'
205° 00'

Figure 1

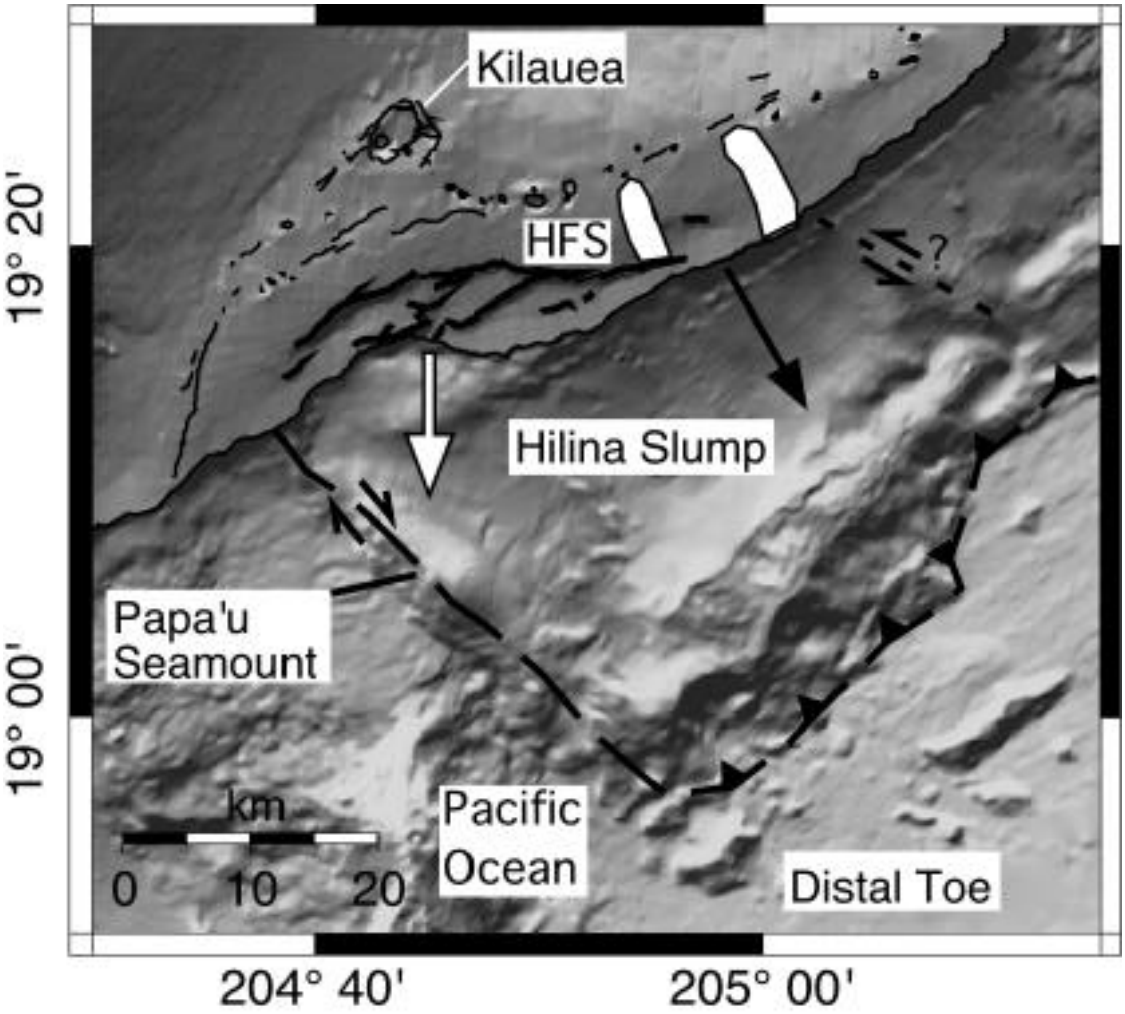
Kilauea
HFS
?
Hilina Slump
Papa'u
Seamount
km
0
10
20
Pacific
Ocean
Distal Toe
19° 20'
19° 00'
204° 40'
205° 00'

Figure 2

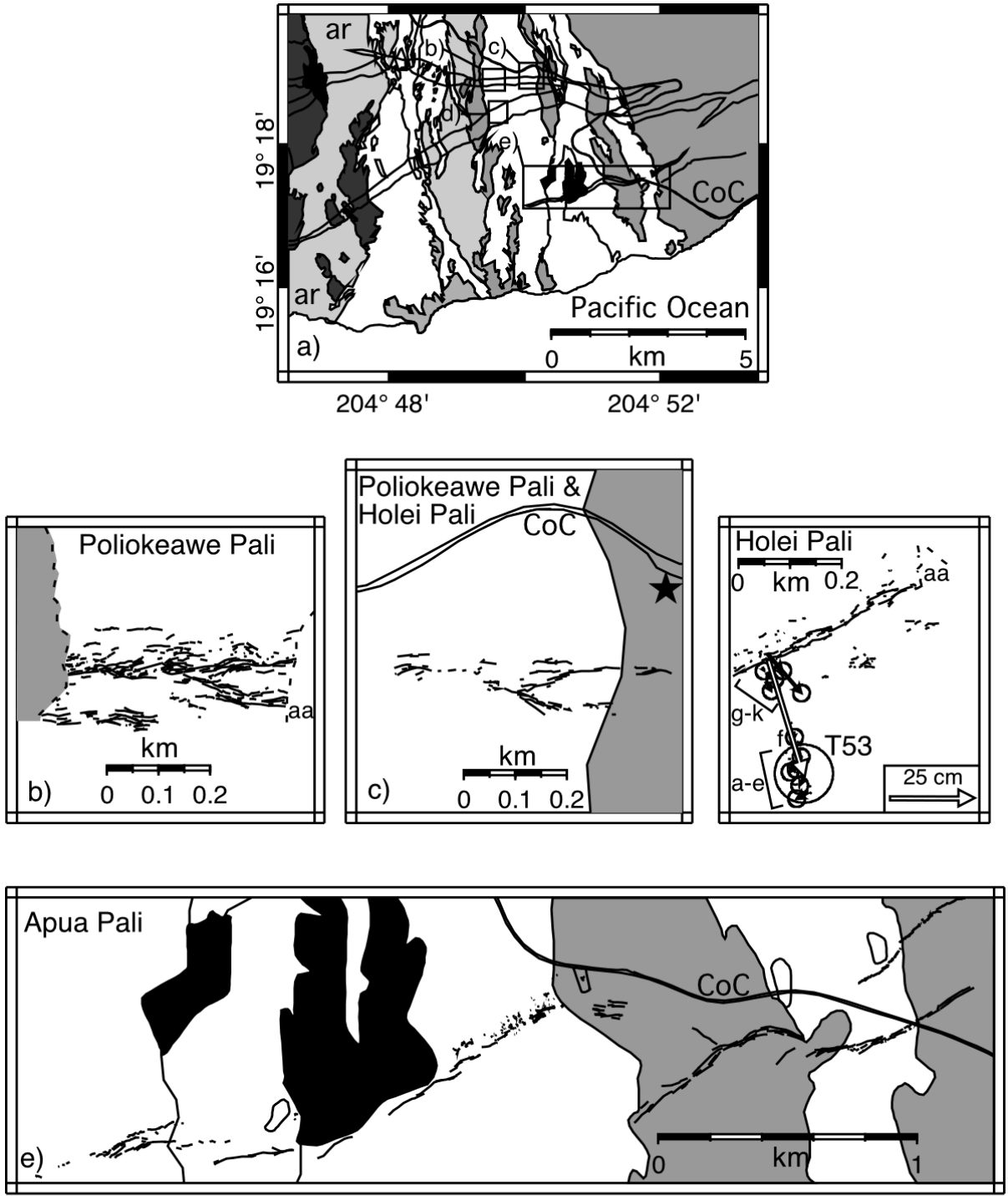
ar
b)
c)
d)
e)
CoC
ar
Pacific Ocean
a)
0 km 5
19° 18'
19° 16'
204° 48'
204° 52'
Poliokeawe Pali
aa
km
b)
0 0.1 0.2
Poliokeawe Pali &
Holei Pali
CoC
km
c)
0 0.1 0.2
Holei Pali
0 km 0.2
aa
g-k
f
T53
a-e
25 cm
Apua Pali
CoC
e)
0 km 1

Figure 3

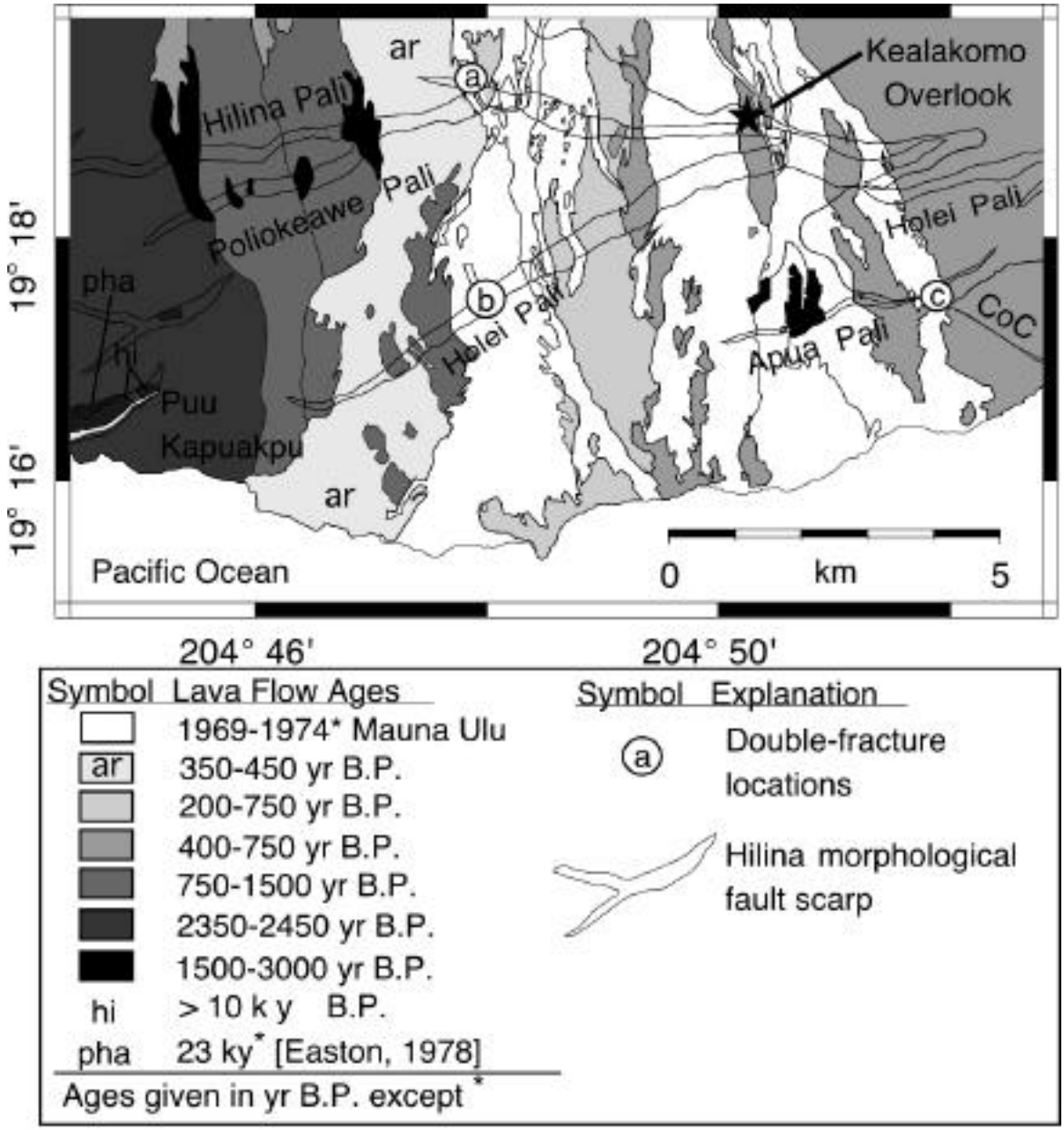
ar
a
Kealakomo
Overlook
Hilina Pali
Poliokeawe Pali
Holei Pali
pha
b
c
CoC
hi
Holei Pali
Apua Pali
Puu
Kapuakpu
ar
19° 18'
19° 16'
Pacific Ocean
0
km
5
204° 46'
204° 50'
Symbol Lava Flow Ages
1969-1974* Mauna Ulu
ar 350-450 yr B.P.
200-750 yr B.P.
400-750 yr B.P.
750-1500 yr B.P.
2350-2450 yr B.P.
1500-3000 yr B.P.
hi > 10 k y B.P.
pha 23 ky* [Easton, 1978]
Ages given in yr B.P. except *
Symbol Explanation
a Double-fracture locations
Hilina morphological fault scarp

Figure 4

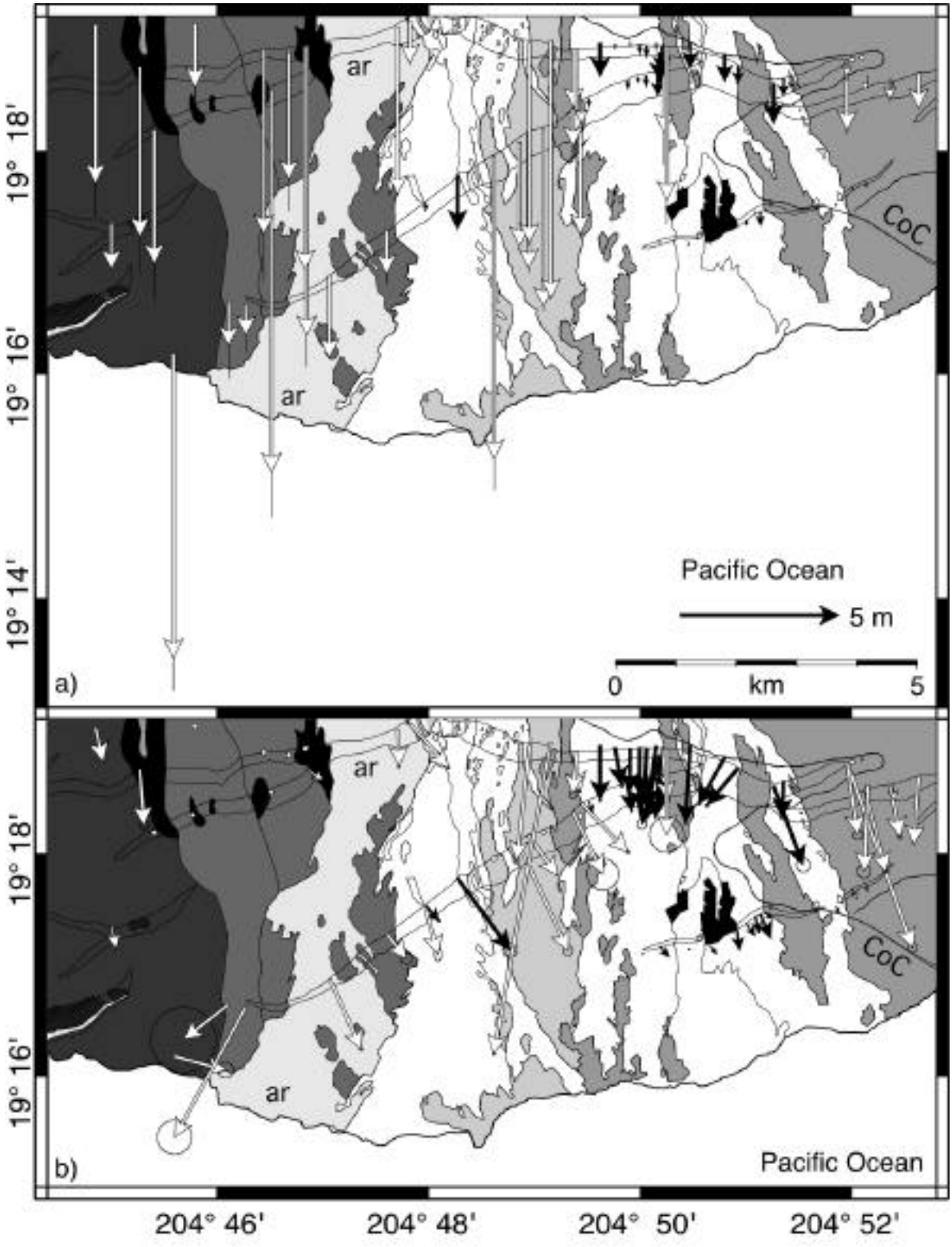
19° 18'
19° 16'
19° 14'
ar
ar
CoC
Pacific Ocean
5 m
0
km
5
a)
19° 18'
19° 16'
ar
ar
CoC
b)
Pacific Ocean
204° 46'
204° 48'
204° 50'
204° 52'

Figure 5

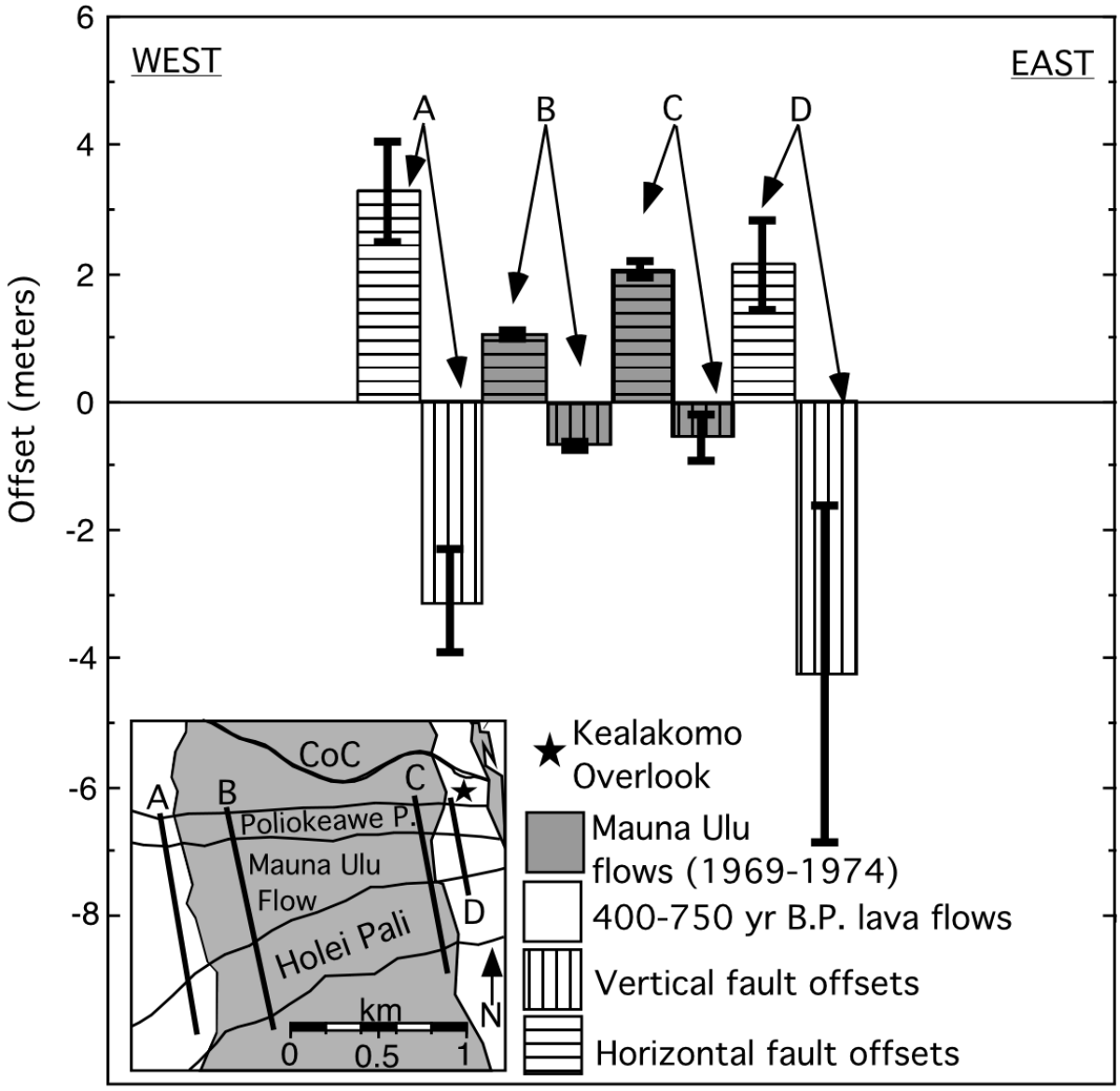
WEST
EAST
A
B
C
D
Offset (meters)
6
4
2
0
-2
-4
-6
-8
CoC
Poliokeawe P.
Mauna Ulu
Flow
Holei Pali
km
0
0.5
1
N
Kealakomo
Overlook
Mauna Ulu
flows (1969-1974)
400-750 yr B.P. lava flows
Vertical fault offsets
Horizontal fault offsets

Figure 6

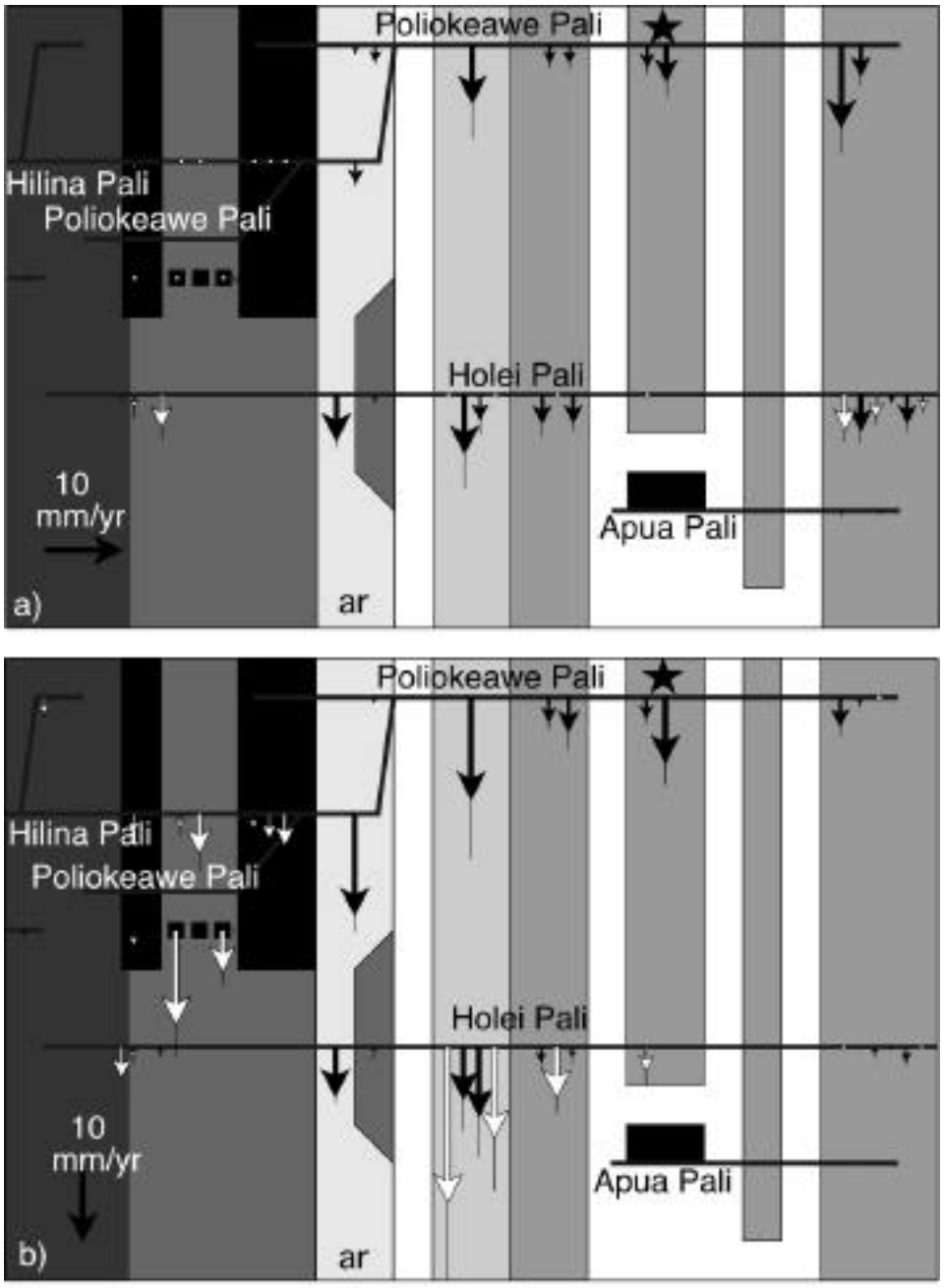
Poliokeawe Pali
Hilina Pali
Poliokeawe Pali
Holei Pali
10
mm/yr
Apua Pali
a)
ar
Poliokeawe Pali
Hilina Pali
Poliokeawe Pali
Holei Pali
10
mm/yr
Apua Pali
b)
ar

Figure 7

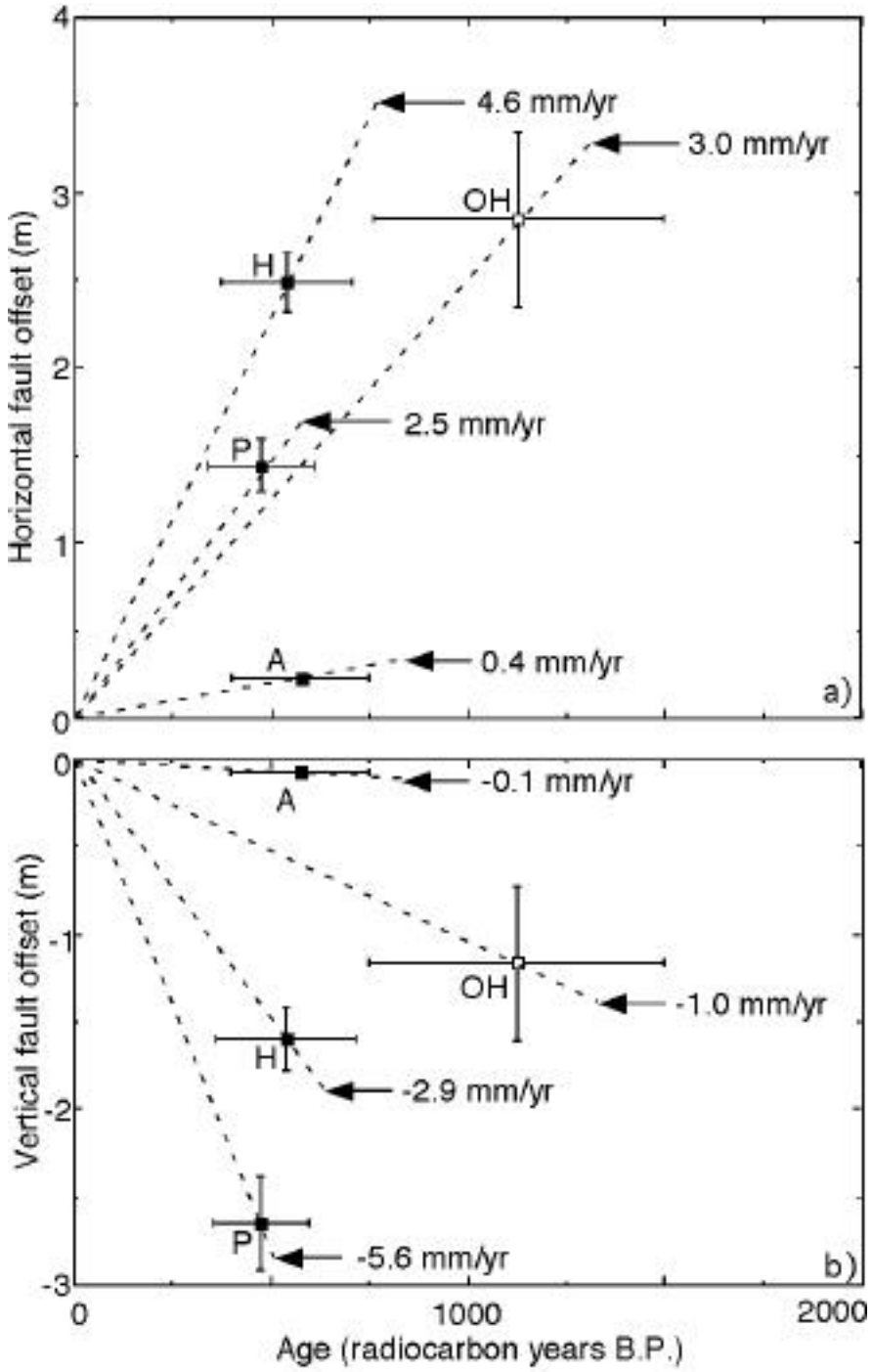
4.6 mm/yr
3.0 mm/yr
OH
H
2.5 mm/yr
P
A
0.4 mm/yr
a)
Horizontal fault offset (m)
-0.1 mm/yr
OH
-1.0 mm/yr
H
-2.9 mm/yr
P
-5.6 mm/yr
b)
Vertical fault offset (m)
Age (radiocarbon years B.P.)

Figure 8

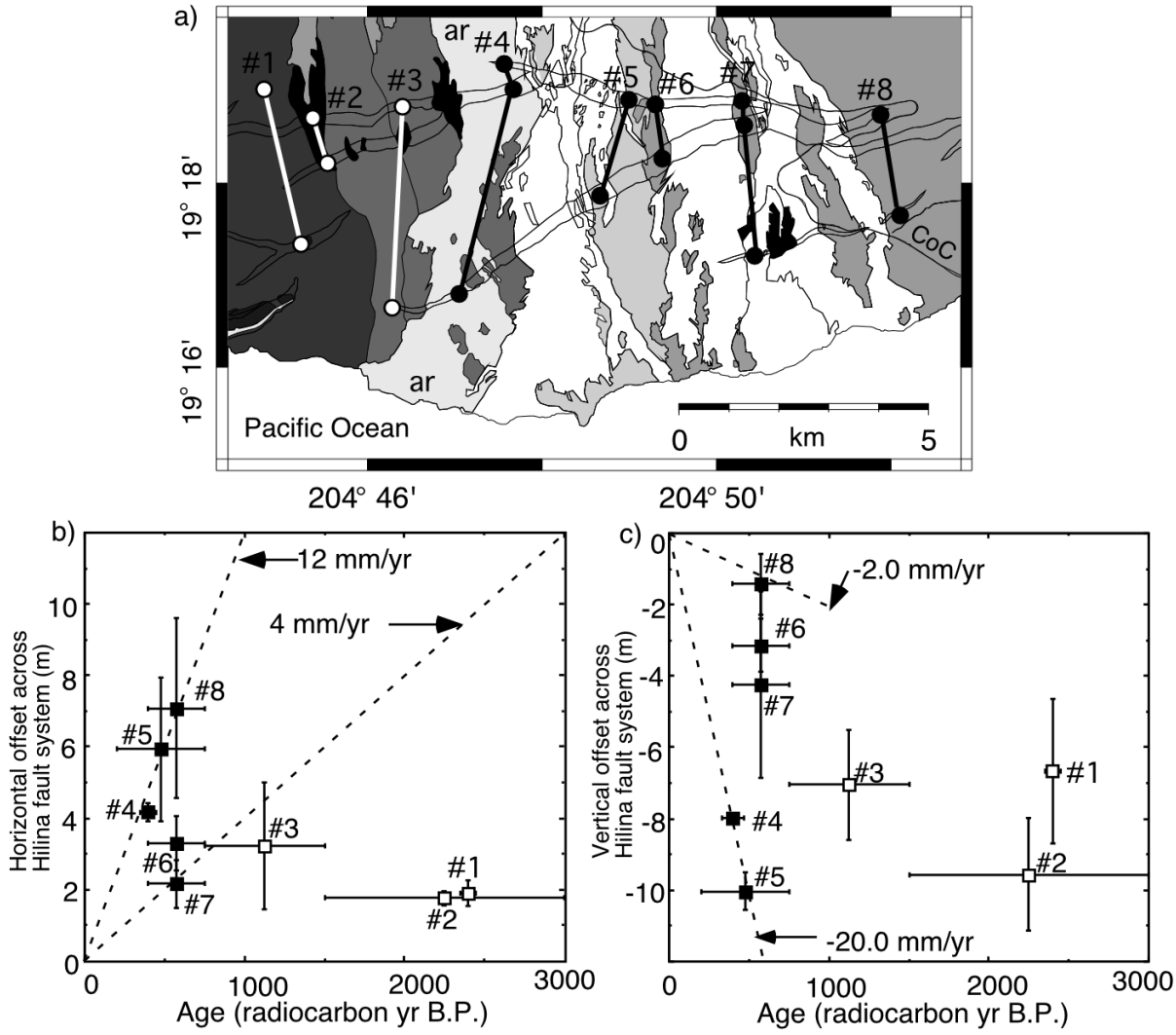
a)
ar
#1
#2
#3
#4
#5
#6
#7
#8
CoC
ar
Pacific Ocean
0
km
5
19° 18'
19° 16'
204° 46'
204° 50'
b)
12 mm/yr
4 mm/yr
Horizontal offset across Hilina fault system (m)
Age (radiocarbon yr B.P.)
c)
-2.0 mm/yr
-20.0 mm/yr
Vertical offset across Hilina fault system (m)
Age (radiocarbon yr B.P.)

Figure 9